Velthuis, J., Page, R., Purves, T., Beck, L., Hanifa, A., & Hugtenburg, R. (2017). Toward Pulse by Pulse Dosimetry Using an SC CVD Diamond Detector. *IEEE Transactions on Radiation and Plasma Medical Sciences*, *1*(6), 527-533. https://doi.org/10.1109/TRPMS.2017.2750799

123 4 5

Towards Pulse by Pulse Dosimetry using a SC CVD diamond detector

J.J. Velthuis, R.F. Page, T.M. Purves, L. Beck, M.A.M. Hanifa and R.P. Hugtenburg

***Abstract*—Solid state detectors with nanosecond response times to incoming radiation are increasingly present at the forefront of radiotherapy dosimetry research. The fast response time of materials, such as diamond, allow pulse by pulse dosimetry. There is a trend in radiotherapy to move towards shorter treatments, using fewer but more intense pulses with varying pulse rates and intensities. This makes the possibility of measuring individual pulses very attractive and would allow intervention during the treatment and not just afterwards. Here an analogue front end has been developed and combined with a CVD diamond detector to provide real time, pulse by pulse beam intensity measurements.The front end design is discussed and the experimental results obtained using a medical LINAC are presented. The results show that the device is capable of pulse by pulse beam intensity measurements up to pulse rates well above 1 kHz. The system performs so well that its variations are negligible compared to the pulse to pulse intensity variations. The dosimetric performance of our system was compared to a commercially available, integrating diamond detector, the microDiamond by PTW. The dose and dose-rate linearity of our system is comparable with the one of the microDiamond and has the additional advantage of being able to measure the deposited dose per pulse.**

***Index Terms*—non-reference dosimetry, small beam dosimetry, synthetic diamond detector**

I. Introduction

EXTERNAL beam radiotherapy (EBRT), used to treat cancer patients, has improved with the development of the medical linear accelerator (LINAC). LINACs are capable of generating both electron and photon beams which are used in treatment delivery. Generally, photon beams consist of a series of pulses with a constant pulse duration of around 4 μs. A range of pulse rate repetition frequencies (PRF) are available depending on the LINAC. PRFs are typically a few hundred Hz and do not exceed 1 kHz. To verify the applied dose to the patient dosimeters are placed on the skin of the patient. Current solid state dosimetry systems integrate the measured charge over the treatment session to verify the applied dose.

As radiotherapy procedures such as modulated arc therapies are getting more common, a need for time-resolved dosimetry methods arises to verify the dose delivery of a medical LINAC on shorter timescales [1], with one example being the development of fast-scintillator based dosimeters [2]–[4]. These systems utilise high atomic number phosphors and as a consequence do not have a tissue-equivalent response, unlike diamond-based dosimeters. Pulse by pulse dosimetry can be achieved using solid state detectors. Here a single crystal chemical vapour deposition diamond sensor (SC CVD) was used as the radiation detector. SC CVD diamonds are excellent detectors for radiotherapy: they are very radiation hard, have a fast response time, are near tissue equivalent and, in contrast to natural diamonds, have a uniform response from sensor to sensor. The performance of single crystal diamond dosimeters has been reported widely, see for example [5]–[9]. To achieve pulse by pulse readout a custom frontend was developed. Measurements were performed with an Elekta Synergy at Singleton Hospital, Swansea to demonstrate the feasibility of pulse by pulse dosimetry.

J.J. Velthuis is with the School of Physics, University of Bristol, Bristol, BS7 1TL, United Kingdom, and also with Swansea University Medical School, Singleton Park, Swansea, SA2 8PP, United Kingdom.

R.F. Page, T.M. Purves and L. Beck are with the School of Physics, University of Bristol, Bristol, BS7 1TL, United Kingdom.

M.A.M. Hanifa is with Swansea University Medical School, Singleton Park, Swansea, SA2 8PP, United Kingdom.

R.P. Hugtenburg is with Swansea University Medical School, Singleton Park, Swansea, SA2 8PP, United Kingdom, with the Department of Medical Physics and Clinical Engineering, Abertawe Bro Morgannwg University Hospital Board, Swansea SA2 4QA and also with the School of Physics, University of Bristol, Bristol, BS7 1TL, United Kingdom.

Manuscript received April 19, 2005; revised August 26, 2015.

II. Analogue Front End

Commercially available detector front ends, such as the systems presented in [10] tend to focus on high count rate, low intensity signals. In a wide range of radiation environments this is ideal. However, during radiotherapy treatments the pulses are intense but the pulse rate rarely exceeds a few hundred Hz. The generated pulse in the 500 μm thick CVD diamond detector, see section III, is a few microseconds long with an amplitude in the order of 1 mA and a repetition rate well below 1 kHz. With this in mind the following front end was designed. It is a classic design: an AC coupled preamp followed by a two-stage shaper resulting in a semi-Gaussian voltage output.

The schematic is presented in figure 1. The detector itself is represented by $I1$. The operational amplifiers used were Texas Instruments TL082BCP, chosen for their fairly fast slew rate. A short summary of the properties of the amplifiers can be found in table I. The bias voltage is provided by the HV source $V1$. A LINAC pulse will cause electrons to flow onto the AC

TABLE I
TABLE OF TL082BCP AMPLIFIER PROPERTIES

Property	Value	Units
Bandwidth	3	MHz
Slew Rate	13	$V\mu s^{-1}$
Maximum Voltage Supply	± 18	V
Operating Temperature	$0 - 70$	°Celsius

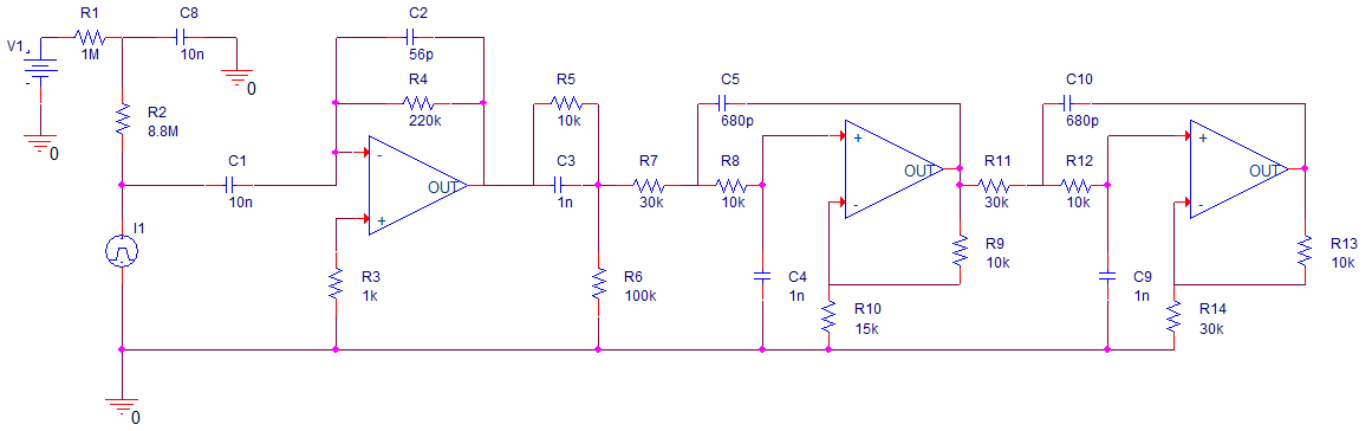

Fig. 1. Circuit diagram of the custom front end constructed. I1 represents a current source, in this case a solid state detector.

decoupling capacitor $C1$. The preamplifier that follows $C1$ is arranged as an operational integrator, with transfer function

$$\frac{v_{out}(s)}{i_{in}(s)} = \frac{R_4}{1 + sR_4C_2} \tag{1}$$

Taking the inverse Laplace transform of this with an impulse of current gives

$$v_{out}(t) = \frac{1}{C_2} e^{-\frac{t}{R_4C_2}} \tag{2}$$

The preamplifier output was passed first to a pole zero cancellation circuit, in order to negate the effects of the pole at $s = -RC$ and provide optimal baseline restoration. It then passes through two Sallen-Key filters [11] in a low pass configuration that act both to filter out high frequency noise in the system and shape the pulse for data acquisition. The transfer function of the first Sallen-Key filter is

$$\frac{v_{out}(s)}{v_{in}(s)} = \frac{w_0^2}{s^2 + 2as + w_0^2} \tag{3}$$

with

$$w_0 = \frac{1}{\sqrt{R_7R_8C_5C_4}} \tag{4}$$

and

$$2a = \frac{R_7 + R_8}{R_7R_8} \tag{5}$$

such that the output pulse from a single stage of shaping can be obtained by taking the inverse Laplace transform. This configuration produces a semi-Gaussian voltage pulse which is slow enough, so that extremely fast and complex data acquisition systems are not needed. Gain control is available by altering the negative feedback resistor pairs R_9 and R_{10}, or R_{13} and R_{14}, following the usual gain control method [12]. The voltage output was measured between the circuit ground and the output of the amplifier used in the second stage of pulse shaping. In this work a National Instruments PCI 6024E DAQ was used to digitise the input signal and readout out the sensor. The DAQ was operating at its maximum acquisition rate of 200 kilo-samples per second, giving 5 μs resolution on the time base. The 6024E card has a 4.88 mV resolution on the voltage base.

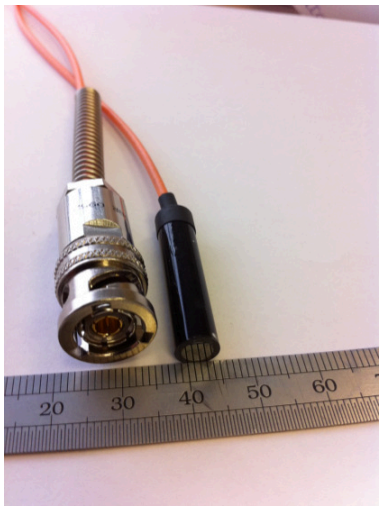

Fig. 2. The encapsulated diamond detector.

III. The SC CVD Diamond Detector

The detector system uses a single crystal CVD diamond purchased from Diamond Detectors Ltd (Poole, U.K.). The detector is encapsulated in a tissue equivalent plastic resin and the sensitive volume is a high-purity single crystal diamond with concentrations of less than 1ppm of boron and nitrogen. The size of the sensitive volume is 1×1 mm^2 and 0.5 mm thick. The bias voltage was 100 V. A picture of the encapsulated diamond detector is shown in figure 2. Figure 3 shows a radiograph of the encapsulated module. The electrical contacts were made through top and bottom pads with a proprietary metalization technique (Diamond Like Carbon/Pt/Au) [13].

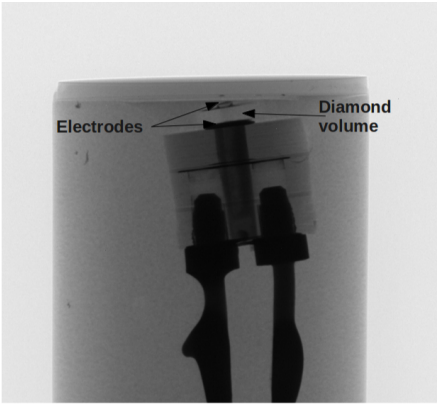

Fig. 3. A radiograph of the encapsulated diamond dectector.

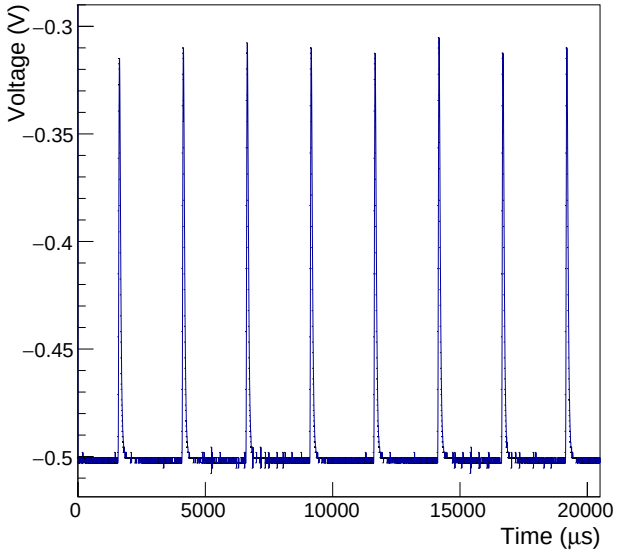

Fig. 4. Example of a pulse train measurement taken with the LINAC operating at 400 MU·min^{-1}.

IV. Experimental set up

Measurements were taken at Singleton Hospital, Swansea using an Elekta Synergy. The LINAC was operated at an acceleration voltage of 6 MV at 400 MU·min^{-1} with a 10×10 cm^2 field size at 100 cm source to surface distance (SSD). The data was recorded during mid-delivery of the beam to avoid any pulse variations due to start up issues of the LINAC. The detector was mounted in a custom built 8×8×8 cm^3 PMMA phantom. The detector is cylindrical and was positioned with its main axis perpendicular to the incoming photon beam. To minimise effects from scattering the cube was shielded on all sides using multiblock RW3 solid water phantoms. The sensor was placed 1.5 cm deep in the phantom: the depth of maximum dose for a 6 MV beam.

V. Results

Figure 4 shows the detector response to a series of LINAC pulses as measured with the described system. A single

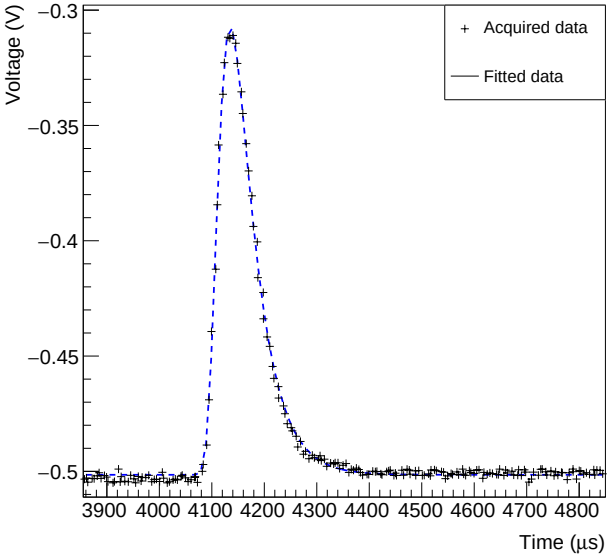

Fig. 5. Example of a measured detector signal pulse taken with the LINAC operating at 400 MU·min^{-1}. The line shows a fit to the data using equation 6.

detector signal pulse is shown in figure 5. The detector signal pulse displays the expected semi-Gaussian behaviour with a rapid rise and slower fall. The detector signal pulse is very well described by the parametrisation

$$V(t) = p_0 e^{-\frac{1}{2}\left(\lambda + e^{-\lambda}\right)} + p_1 \qquad \lambda = \frac{t - p_2}{p_3} \tag{6}$$

where the parameters p_i are extracted from the fit. The fit, also shown in figure 5, was performed using the ROOT package [14]. From the fit, the peak height and the integral of the signal pulse, which is a measure of the charge of the signal pulse and thus of the dose in patient per LINAC pulse, are extracted.

It is an important design criterium that the front end pulse is fast enough such that signal returns to baseline before the next LINAC pulse arrives. If the next LINAC pulse would arrive before the signal has returned to 0, signal pulse pile up occurs. The pile up will lead to an increased base line for subsequent measurements of the detector signal. In principle this can be corrected for offline until the detector signal reaches the maximum of the dynamic range. This would make dosimetry impossible. To study whether pile up is a problem the signal pulse duration, defined as the time the signal pulse exceeded a certain fraction of the peak height, was extracted from the data for 2% and 5% of the peak height as a function of the SSD. Figure 6 demonstrates that the pulse duration does not depend on the dose rate. In addition, the pulse duration was calculated for 5%, 2%, 1% and 0.1% of the peak height. The calculations for 5% and 2% agree well with the data. The calculated pulse duration time for 0.1% of the peak height is 365.7 μs. Hence, there is no problem with signal pulse pile up as long as the PRF does not exceed 2734 Hz. Since medical operation rarely exceeds 400 Hz, the

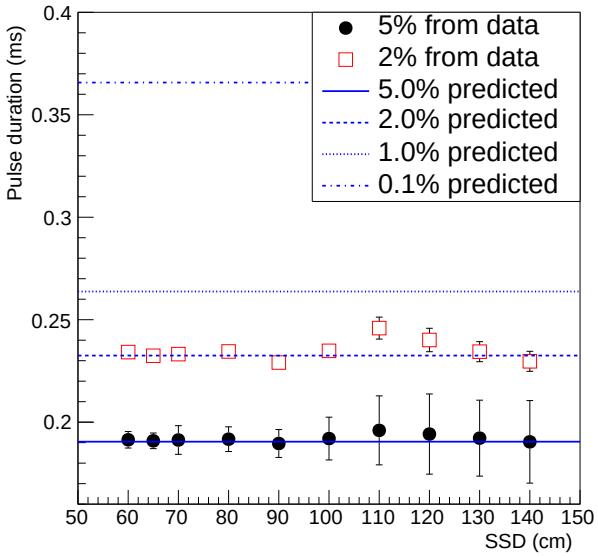

Fig. 6. The detector signal pulse duration, defined as the time the signal pulse exceeded a certain fraction of the peak height, measured for 2% and 5% of the peak height as a function of the SSD and the predicted values for 5%, 2%, 1% and 0.1% of the peak height.

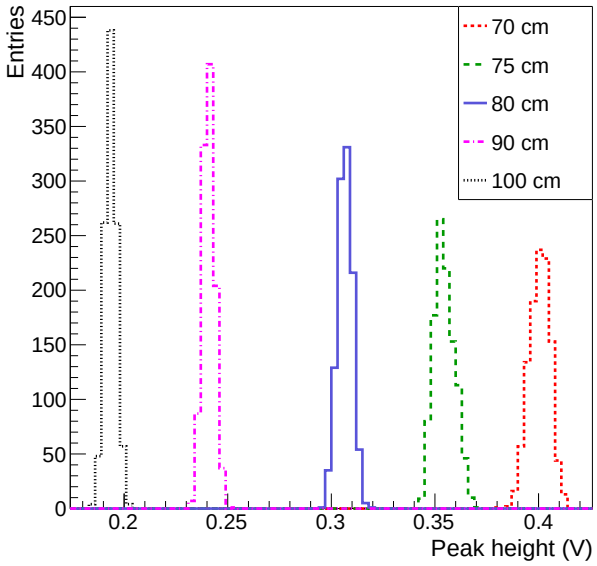

Fig. 7. The distribution of the peak height of the detector signal for several SSD values: from left to right the SSD was 100, 90, 80, 75 and 70 cm.

effects of signal pulse pile up can be safely neglected. This is essential to perform pulse by pulse dosimetry effectively.

The LINAC producing the X-rays is effectively a point source. This is a well assessed model in external beam radiation dosimetry, see for example [15]. The energy absorbed by a detector at the point of maximum dose in the phantom is expected to closely follow the inverse square law as a function of the source to the detector distance. To vary the signal per pulse the SSD was varied. The distribution of the peak height of the charge per pulse as a function of the SSD is shown in figure 7. The peak height of the charge per pulse is proportional to the total charge per pulse as will be shown later on in this section. Figure 8 shows the average charge per pulse as a function of the SSD. The data was fitted using the inverse square law with an offset a for the depth at which the measurement was performed

$$Q_{pulse} = \frac{Q_{LINAC}}{(SSD - a)^2} \tag{7}$$

to correct the SSD where Q_{pulse} is the measured average charge per pulse and Q_{LINAC} the average charge emitted by the LINAC per pulse. As can be seen in figure 8, the data is well described by the inverse square law including the offset. The obtained value for a of -1.7±0.4 cm corresponds well to the calibrated depth of 1.5 cm.

Figure 7 demonstrates that the measured charge per pulse varies for each SSD. Part of this will be due to the pulse to pulse intensity variation of the LINAC and part due to imperfections in our measurement and analysis chain. As demonstrated in figure 8 the measured intensity follows the

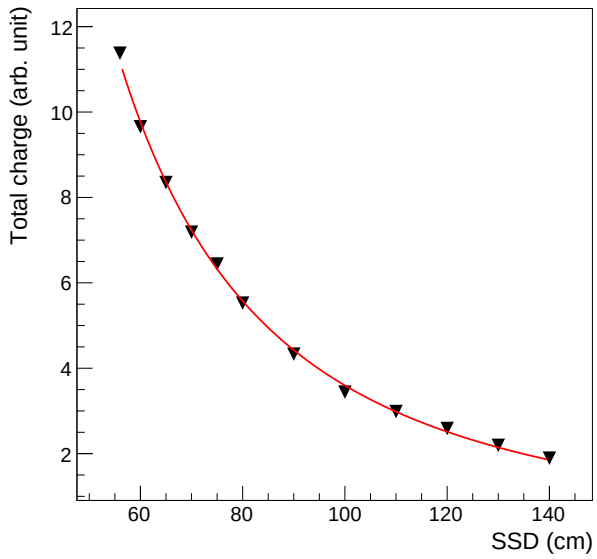

Fig. 8. The measured average charge per pulse in the detector in arbitrary units as a function of the SSD, along with an inverse square fit to the data.

expected inverse square law. Any pulse to pulse variation in our measured signal will therefore lead to an inverse square dependence of the standard deviation of the measured charge per pulse. It is reasonable to assume that the component of the standard deviation due to our measurement system is independent of the SSD as the measured pulse heights are quite small compared to the maximum input range. Therefore, the standard deviation as a function of the SSD should follow

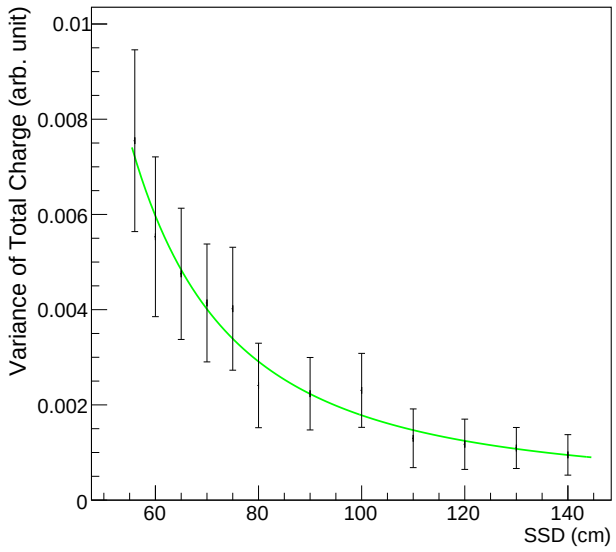

Fig. 9. Variance of the measured pulse charge as a function of the SSD.

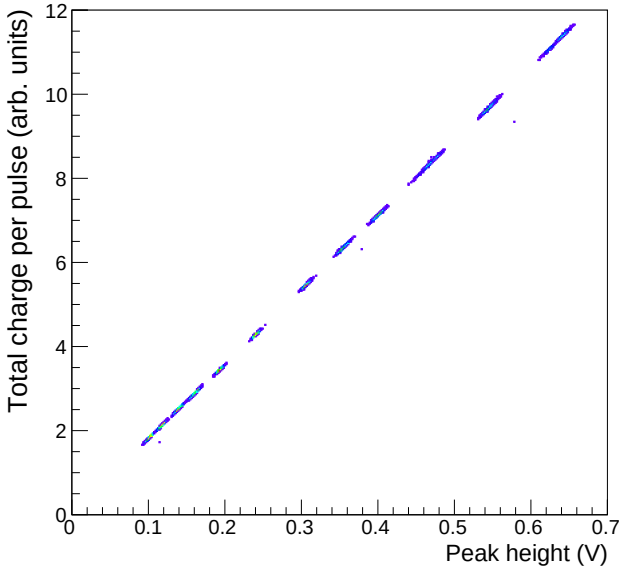

Fig. 10. The total charge per pulse as a function of the pulse peak height for pulses measured at several SSD values.

the parametrisation given in equation 8

$$\sigma^2_{overall}(SSD) = \frac{\alpha}{(SSD - a)^2} + \beta \tag{8}$$

where β is the standard deviation squared due to our measurement system. The fit of equation 8, shown in figure 9, describes the data well. From the fit β was extracted to be $(0.3 \pm 0.7) \times 10^{-3}$, which is compatible with 0. Furthermore, at a SSD of 140 cm where the smallest standard deviation was measured, the value was approximately 0.03 which is an order of magnitude larger than the obtained value for β. Hence, the imperfections in our measurement and analysis chain are negligible and the measured pulse to pulse variation is due to actual pulse to pulse intensity variations of the LINAC.

For practical applications, it would be desirable if pulse fitting is not required as it takes time to execute and requires storing a significant amount of data per pulse. In figure 10 the pulse integral is plotted as a function of the peak height. The figure shows that the integral is directly proportional to the peak height. Fitting figure 10 with a straight line yielded a slope of 17.7 ± 0.5 and an offset of 0.04 ± 0.2 which is compatible with 0, demonstrating that the peak height is indeed proportional to the pulse height. Hence, it is sufficient to extract the peak height per pulse. This can be easily done either in the electronics, firmware or offline.

VI. Comparison with microDiamond

The performance of our device was compared to a commercially available diamond detector system, the microDiamond type 60019 by PTW [16]. The microDiamond is a commercial diamond detector system in Schottky diode configuration; no external bias voltage is required. The detector has an active volume of 0.004 mm^3 and the effective point of measurement from the tip is 1 mm. The microDiamond system was connected to a PTW UNIDOS dosimeter to measure the charge generated by the photon beams. Several studies on the use of this system in therapeutic dosimetry have been reported [17]–[20].

In radiotherapy it is common to compare detector systems after normalisation to the deposited dose (or signal) at a calibrated depth. Here, the phantom surface was at 100 cm SSD and the measurement was done at a depth of 1.5cm in RW3 Solid Water using a 6 MV beam. Figure 11 shows the normalised average total charge per pulse for the DDL SC CVD diamond system and the PTW microDiamond system as a function of the source to detector distance. The agreement between the two detector systems is very good. As mentioned before, the normalised average total charge per pulse as a function of the source to detector distance should follow an inverse square law function. To verify this a fit was performed for both detectors using the parametrisation

$$y = Ax^b \tag{9}$$

For the DDL SC CVD diamond, the obtained parameter values were $A = (1.01 \pm 0.09) \times 10^4$ cm^{-1} and $b = (-2.00 \pm 0.02)$. For the microDiamond the obtained parameter values were $A = (0.982 \pm 0.005) \times 10^4$ cm^{-1} and $b = (-1.990 \pm 0.001)$. The fit results showed that both detectors agree very well with the expected inverse square law. Furthermore, the fit results confirm that both systems agree very well with each other as both fit parameters are within errors the same for both systems, although the uncertainties for the DDL SC CVD diamond system are an order of magnitude worse. However, the errors for both systems are very small.

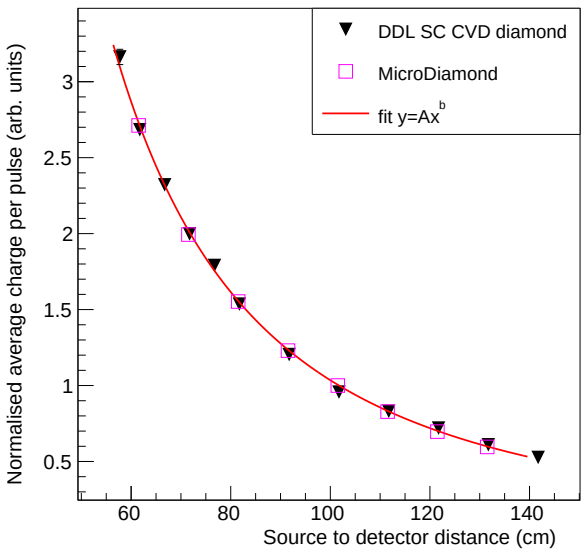

Fig. 11. Normalised average total charge per pulse for the DDL SC CVD diamond system and the PTW microDiamond system as a function of the source to detector distance. For clarity only the fit for the DDL SC CVD diamond is shown.

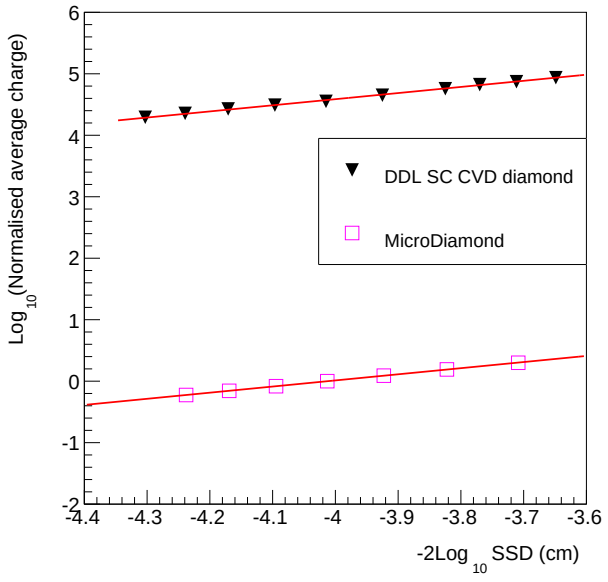

Fig. 12. The logarithm of the average total charge per pulse for the DDL SC CVD diamond system and the PTW microDiamond as a function of the SSD.

The microDiamond has previously been demonstrated to have excellent dose-rate linearity [17]. To compare the dose-rate linearity of the DDL SC CVD diamond system with the PTW microDiamond system, the logarithm of the average total charge per pulse was plotted as a function of the SSD, see figure 12. This allowed the Fowler factor for both detectors to be extracted as the slope of a linear fit. The measured Fowler factor for the PTW microDiamond system was (0.9964±0.0004) which agrees well with the value reported in [21] of (0.999±0.07%). The Fowler factor for the DDL SC CVD diamond system was found to be (0.996±0.025) which agrees well with the PTW microDiamond system. From the above it follows that the performance of our system is similar to the performance of the microDiamond system in terms of dose-rate linearity. This is a remarkable result for the DDL SC CVD diamond detector system as this contains a thick, biased diamond detector, with a much larger sensitive volume, in contrast a microDiamond, which contains a thin Schottky diode. Schottky diodes are expected to have very good linearity. Dose-rate linearities have been measured in single-crystal CVD diamond detectors by a number of groups [6], [9], [22]–[28], several of whom determined a significant non-linear response as a function of dose-rate [6], [9], [23], [27], [28]. A variety of methodologies were used, including varying the PRF, varying the source current in the case of X-ray sources, and varying the source to detector distance, which is the method that has been used here. We expect that our good dose rate linearity is due to our improved pulse handling. The advantage of using the DDL SC CVD diamond detector system compared to microDiamond system is that our system measures the dose per pulse and not the integral dose over the treatment. This is important for dynamic treatments like VMAT and IMRT.

VII. Conclusion

We have successfully demonstrated pulse by pulse beam intensity measurements on a medical LINAC using a 500 μm thick SC CVD diamond sensor inside a phantom, which was read out using a simple, custom built front end. The front end is a classic design using a preamp and a two stage Sallen-Key filter. We have shown that individual pulses can be measured using this system, up to pulse rates of well above 1 kHz. The measured peak pulse heights are proportional to the amount of measured charge. Hence, it is sufficient to extract the peak height per pulse. This can be easily done either in the electronics, firmware or offline. Our system performs so well that the imperfections in our measurement and analysis chain are negligible compared to the actual pulse to pulse intensity variations over a large range of pulse amplitudes. The performance of our system was compared to a commercially available diamond detector system, the microDiamond by PTW. The comparison study shows that the performance of our system is similar in terms of dose-rate linearity to the performance of the microDiamond. This is a remarkable result for the DDL SC CVD diamond dosimetry system as dose-rate linearity for other conductivity detectors is in general much poorer than the dose-rate linearity for Schottky diode systems, like the microDiamond. Furthermore, the system presented here has the advantage that the deposited dose is measured for each pulse, which is important for dynamic treatments. Hence, pulse by pulse dosimetry on medical LINACs is entirely feasible during treatments using this system.

REFERENCES

[1] A. Ravnsborg Beierholm, Pulse-resolved radiotherapy dosimetry using fiber-coupled organic scintillators, PhD thesis, Technical Univ. of Denmark, (2011).

[2] A.R. Beierholm, C.E. Andersen, L.R. Lindvold & M.C. Aznar, 2010. Investigation of linear accelerator pulse delivery using fast organic scintillator measurements. Radiation Measurements, 45(3), pp.668-670.

[3] S. OKeeffe, W. Zhao, W. Sun, D. Zhang, Z. Qin, Z. Chen, Y. Ma & E. Lewis, 2016. An optical fibre-based sensor for real-time monitoring of clinical linear accelerator radiotherapy delivery. IEEE Journal of Selected Topics in Quantum Electronics, 22(3), pp.35-42.

[4] M.C. Aznar, C.E. Andersen, L. Botter-Jensen, S.A.J. Back, S. Mattsson, F. Kjaer-Kristoffersen and J. Medin, 2004. Real-time optical-fibre luminescence dosimetry for radiotherapy: physical characteristics and applications in photon beams. Physics in medicine and biology, 49(9), pp.1655-1670

[5] F. Marsolat et al, A new single crystal diamond dosimeter for small beam: comparison with different commercial active detectors, Phys. Med. Biol. 58 (2013) 76477660

[6] M.A. Piliero, R.P. Hugtenburg, S.J.S. Ryde and K. Oliver, Development of CVD diamond detectors for clinical dosimetry, Radiation Physics and Chemistry, Volume: 104, Pages: 10 - 14 (2015)

[7] M. Pimpinella et al, A synthetic diamond detector as transfer dosimeter for Dw measurements in photon beams with small field sizes, Metrologia, Volume 49, Number 5 (2012).

[8] F. Marsolat et al, Diamond dosimeter for small beam stereotactic radiotherapy, Diamond and Related Materials, Volume 33, March 2013, Pages 6370.

[9] C.M. Buttar, J. Conway, R. Meyfarth, G. Scarsbrook, P.J. Sellin, A. Whitehead, CVD diamond detectors as dosimeters for radiotherapy, Nucl. Instr. and Meth. A 392 (1997) 281-284.

[10] M. Fisher-Levine, J. Velthuis, D. Cussans and S. Nash, A Fast Analogue Front End for a Diamond Radiation Spectrometer, , IEEE Transactions on Nuclear Science, vol. 60, no. 5, pp. 3990-3994, (2013)

[11] J. Karki, Active low-pass filter design, Texas Instruments Application Report, (2000)

[12] B. Carter and T.R. Brown,*Handbook of operational amplifier applications. Vol. 9*, Texas Instruments, (2001)

[13] A. Galbiati, S. Lynn, K. Oliver, F. Schirru, T Nowak, B Marczewska, J.A. Dueas, R. Berjillos, I. Martel & L. Lavergne, Performance of monocrystalline diamond radiation detectors fabricated using TiW, Cr/Au and a novel ohmic DLC/Pt/Au electrical contact. IEEE Transactions on Nuclear Science, 56(4), 1863-1874.

[14] ROOT Data Analysis Framework, available from https://root.cern.ch

[15] Khan, F.M. and Gibbons, J.P., 2014. Khan's the physics of radiation therapy. Lippincott Williams & Wilkins.

[16] microDiamond: synthetic diamond detector for high-precision dosimetry. Freiburg, Germany: PTW-Freiburg 2013, http://www.ptw.de/2732.html

[17] I. Ciancaglioni et al, Dosimetric characterization of a synthetic single crystal diamond detector in clinical radiation therapy small photon beams, Med.Phys.39(2012), 4493-501

[18] L. Brualla-Gonzalez, F. Gomez, M. Pombar and J. Pardo-Montero, Dose rate dependence of the PTW60019 microDiamond detector in high dose-per-pulse pulsed beams. Phys.Med.Biol. 61(2016)N11-N19

[19] J.E. Morales, S.B. Crowe, R. Hill, N. Freeman, J.V. Trapp, Dosimetry of cone-defined stereotactic radiosurgery fields with a commercial synthetic diamond detector, Med Phys. 2014 Nov;41(11):111702

[20] W. Laub, R. Crilly, Clinical radiation therapy measurements with a new commercial synthetic single crystal diamond detector, Journal of applied medical physics, Vol 15, No 6, 2014.

[21] J.M. Lárraga-Gutiérrez, P.B. Ballesteros-Zebadúa, M. Rodríguez-Ponce, O.A. garcía-Garduño and O. Olinca Galván de la Cruz, Properties of a commercial PTW-60019 synthetic diamond detector for the dosimetry of small radiotherapy beams, Phys. Med. Biol. 60 (2015) 905924.

[22] N. Tranchant, D. Tromson, C. Descamps, A. Isambert, H. Hamrita, P. Bergonzo, M. Nesladek High mobility single crystal diamond detectors for dosimetry: Application to radiotherapy, Diamond & Related Materials 17(2008) 1297-1301.

[23] D. Tromson, C. Descamps, N. Tranchant, P. Bergonzo, M. Nesladek and A. Isambert, Investigations of high mobility single crystal chemical vapor deposition diamond for radiotherapy photon beam monitoring, Journal of Applied Physics, 054512 (2008).

[24] C. Descamps, D. Tromson, N. Tranchant, A. Isambert, A.Bridier, C. De Angelis, S. Onori, M. Bucciolini, P. Bergonzo, Clinical studies of optimised single crystal and polycrystalline diamonds for radiotherapy dosimetry, Radiation Measurements 43 (2008) 939-938.

[25] S.P. Lansley, G.T. Betzel, F. Baluti, L. Reinisch and J Meyer, Investigate of the suitability of commercially available CVD diamond for megavoltage X-ray dosimetry, Nuclear Instruments and Methods in Physics Research A 607 (2009)659-667.

[26] A. Galbiati, S. Lynn, K.Oliver, F. Schirru, T. Nowak, B. Marczewska, J. A.Duenas, R. Berjillos, I. Martel and L. Lavergne, Performance of Monocrystalline Diamond Radiation Detectors Fabricated Using TiW, Cr/Au and a Novel Ohmic DLC/Pt/Au Electrical Contact, IEEE Transactions on Nuclear Science, Vol. 56,No 4, August 2009

[27] F. Schirru, K. Kisielewicz, T. Nowak, B. Marczewska, Single crystal diamond detector for radiotherapy, Journal of Physics D: Applied Physics, IOP Publishing , 2010, 43(26).

[28] F. Marsolat, D. Tromson, N. Tranchant, M. Pomorski, D.Lazaro-Ponthus, C. Bassinet, C. Huet, S. Derreumaux, M. Chea, G. Boisserie, J. Alvarez, P. Bergonzo, Diamond dosimeter for small beam stereotactic radiotherapy, Diamond & Related Materials 33(2013) 63-70.